Asian Journal of Chemistry; Vol. 27, No. 10 (2015), 3539-3542

ASIAN JOURNAL OF CHEMISTRY

http://dx.doi.org/10.14233/ajchem.2015.18715

Synthesis of $NaGd(MoO_4)_2:Eu^{3+}/Yb^{3+}$ Phosphors by Cyclic Microwave-Modified Sol-Gel Method and their Upconversion Photoluminescence Properties

CHANG SUNG LIM

Department of Advanced Materials Science and Engineering, Hanseo University, Seosan 356 706, Republic of Korea

Corresponding author: Tel/Fax: +82 41 6601445; E-mail: cslim@hanseo.ac.kr

Received: 8 September 2014; *Accepted*: 28 November 2014; *Published online*: 22 June 2015; AJC-17297

$NaGd_{1-x}(MoO_4)_2:Eu^{3+}/Yb^{3+}$ phosphors with doping concentrations of Eu^{3+} and Yb^{3+} ($x = Eu^{3+} + Yb^{3+}$, $Eu^{3+} = 0.05$, 0.1, 0.2 and $Yb^{3+} = 0.2$, 0.45) were successfully synthesized by the microwave-modified sol-gel method and the upconversion and spectroscopic properties were investigated. Well-crystallized particles showed a fine and homogeneous morphology with particle sizes of 2-5 μm. Under excitation at 980 nm, in the case of $NaGd_{0.5}(MoO_4)_2:Eu_{0.05}Yb_{0.45}$ the particles exhibited a strong 525 nm emission band and a weak 550 nm emission band in the green region and a very weak 615 nm emission band in the red region. In the case of $NaGd_{0.7}(MoO_4)_2:Eu_{0.1}Yb_{0.2}$ the particles showed a strong 475 nm emission band in the blue region and a strong 525 nm and a weak 550 nm emission bands in the green region. The Raman spectra of the doped particles indicated the domination of strong peaks at higher frequencies of 780, 890, 1366 and 1438 cm^{-1} and at lower frequencies of 324 and 400 cm^{-1}.

Keywords: Phosphors, Microwave sol-gel, Upconversion, Raman spectroscopy.

INTRODUCTION

White light-emitting diodes (LED) is promising light source due to its advantages, including low power consumption, low voltage, long service life, high reliability, environmental friendliness and high efficiency. The trichromatic phosphors based on blue, green and red phosphors play an important role to adjust chromogenic performance for the application of near-UV light-emitting diodes chips[1,2]. Rare-earth activated upconversion (UC) particles can convert near infrared radiation of low energy into visible radiation of high energy. Recently, the synthesis and the luminescence properties of upconversion particles have attracted considerable interest since they are considered as potentially active components in new optoelectronic devices and luminescent labels for imaging and biodetection assays, which overcome the current limitations in traditional photoluminescence materials[3]. The double molybdate compounds of $MRe(MoO_4)_2$ belong to a group of double alkaline earth lanthanide molybdates. With the decrease in the ionic radius of alkaline earth metal ions, it is possible for the structure of $MRe(MoO_4)_2$ to be transformed to a highly disordered tetragonal Scheelite structure from the monoclinic structure. It is possible for the trivalent rare earth ions in the disordered tetragonal-phase to be partially substituted by Eu^{3+} and Yb^{3+} ions, these ions are effectively doped into the crystal lattices of the tetragonal phase due to the similar radii of the trivalent rare-earth ions in Re^{3+}, resulted in the excellent upconversion photoluminescence properties[4-6]. Among rare-earth ions, the Eu^{3+} ion is suitable for converting infrared to visible light through the upconversion process due to its appropriate electronic energy level configuration. The co-doped Yb^{3+} ion and Eu^{3+} ion can remarkably enhance the upconver-sion efficiency for the shift from infrared to visible light due to the efficiency of the energy transfer from Yb^{3+} to Eu^{3+}. The Yb^{3+} ion, as a sensitizer, can be effectively excited by an incident light source energy. This energy is transferred to the activator from which radiation can be emitted[7-9].

Rare-earth activated double molybdates has attracted great attention because of the spectroscopic characteristics and excellent upconversion photoluminescence properties. Several processes have been developed to prepare these rare-earth doped double molybdates.

Usually, the sol-gel process provides some advantages over the conventional solid-state method, including good homogeneity, low calcination temperature, small particle size and narrow particle size distribution optimal for good luminescent characteristics. However, the sol-gel process has a disadvantage in that it takes a long time for gelation. As compared with the usual methods, microwave-modified sol-gel synthesis has the advantages of very short reaction time, homogeneous morphology features and high purity of final polycrystalline samples[10-12]. Microwave heating is delivered to the material

surface by radiant and/or convection heating, which is transferred to the bulk of the material *via* conduction[13,14]. A cyclic microwave-modified sol-gel process is a cost-effective method that provides high homogeneity with easy scale-up and it is emerging as a viable alternative approach for the synthesis of high-quality luminescent materials in short time periods.

In this study, $NaGd_{1-x}(MoO_4)_2:Eu^{3+}/Yb^{3+}$ phosphors with doping concentrations of Eu^{3+} and Yb^{3+} ($x = Eu^{3+} + Yb^{3+}$, $Eu^{3+} = 0.05, 0.1, 0.2$ and $Yb^{3+} = 0.2, 0.45$) phosphors were prepared by the cyclic microwave-modified sol-gel method followed by heat treatment. The synthesized particles were characterized by X-ray diffraction (XRD), scanning electron microscopy (SEM) and energy-dispersive X-ray spectroscopy (EDS). The optical properties were examined comparatively using photoluminescence (PL) emission and Raman spectroscopy.

EXPERIMENTAL

Appropriate stoichiometric amounts of $Na_2MoO_4{\cdot}2H_2O$ (99 %, Sigma-Aldrich, USA), $Gd(NO_3)_3{\cdot}6H_2O$ (99 %, Sigma-Aldrich, USA), $(NH_4)_6Mo_7O_{24}{\cdot}4H_2O$ (99 %, Alfa Aesar, USA), $Eu(NO_3)_3{\cdot}5H_2O$ (99.9 %, Sigma-Aldrich, USA), $Yb(NO_3)_3{\cdot}5H_2O$ (99.9 %, Sigma-Aldrich, USA), citric acid (99.5 %, Daejung Chemicals, Korea), NH_4OH (A.R.), ethylene glycol (A.R.) and distilled water were used to prepare $NaGd(MoO_4)_2$, $NaGd_{0.8}(MoO_4)_2:Eu_{0.2}$, $NaGd_{0.7}(MoO_4)_2:Eu_{0.1}Yb_{0.2}$ and $NaGd_{0.5}(MoO_4)_2:Eu_{0.05}Yb_{0.45}$ compounds with doping concentrations of Eu^{3+} and Yb^{3+} ($Eu^{3+} = 0.05, 0.1, 0.2$ and $Yb^{3+} = 0.2, 0.45$). To prepare $NaGd(MoO_4)_2$, 0.2 mol % $Na_2MoO_4{\cdot}2H_2O$ and 0.114 mol % $(NH_4)_6Mo_7O_{24}{\cdot}4H_2O$ were dissolved in 20 mL of ethylene glycol and 80 mL of 5M NH_4OH under vigorous stirring and heating. Subsequently, 0.4 mol % $Gd(NO_3)_3{\cdot}6H_2O$ and citric acid (with a molar ratio of citric acid to total metal ions of 2:1) were dissolved in 100 mL of distilled water under vigorous stirring and heating. Then, the solutions were mixed together under vigorous stirring and heating at 80-100 °C. At the end, highly transparent solutions were obtained and adjusted to pH = 7-8 by the addition of NH_4OH or citric acid. In order to prepare $NaGd_{0.8}(MoO_4)_2:Er_{0.2}$, the mixture of 0.32 mol % $Gd(NO_3)_3{\cdot}6H_2O$ with 0.08 mol % $Eu(NO_3)_3{\cdot}5H_2O$ was used for the creation of the rare earth solution.

In order to prepare $NaGd_{0.7}(MoO_4)_2:Eu_{0.1}Yb_{0.2}$, the mixture of 0.28 mol % $Gd(NO_3)_3{\cdot}6H_2O$ with 0.04 mol % $Eu(NO_3)_3{\cdot}5H_2O$ and 0.08 mol % $Yb(NO_3)_3{\cdot}5H_2O$ was used for the rare earth solution.

In order to prepare $NaGd_{0.5}(MoO_4)_2:Eu_{0.05}Yb_{0.45}$, the rare earth containing solution was prepared using 0.2 mol % $Gd(NO_3)_3{\cdot}6H_2O$ with 0.02 mol % $Eu(NO_3)_3{\cdot}5H_2O$ and 0.18 mol % $Yb(NO_3)_3{\cdot}5H_2O$.

The transparent solutions were placed into a microwave oven operating at a frequency of 2.45 GHz with a maximum output-power of 1250 W for 0.5 h. The working cycle of the microwave reaction was controlled precisely using a regime of 40 s on and 20 s off for 15 min, followed by further treatment of 30 s on and 30 s off for 15 min. The samples were treated with ultrasonic radiation for 10 min to produce a light yellow transparent sol. After this, the light yellow transparent sols were dried at 120 °C in a dry oven to obtain black dried gels. The black dried gels were grinded and heat-treated at 900 °C for 16 h with 100 °C intervals between 600-900 °C. Finally, white particles were obtained for $NaGd(MoO_4)_2$ and pink particles for the doped compositions.

The phase composition of the synthesized particles was identified using XRD (D/MAX 2200, Rigaku, Japan). The microstructure and surface morphology of the synthesized aaza particles were observed using SEM/EDS (JSM-5600, JEOL, Japan). The PL spectra were recorded using a spectrophotometer (Perkin Elmer LS55, UK) at room temperature. Raman spectroscopy measurements were performed using a LabRam Aramis (Horiba Jobin-Yvon, France). The 514.5 nm line of an Ar ion laser was used as the excitation source and the power on the samples was kept at 0.5 mW.

RESULTS AND DISCUSSION

Fig. 1 shows the X-ray diffraction patterns of the (a) JCPDS 25-0828 data of $NaGd(MoO_4)_2$, the synthesized (b) $NaGd(MoO_4)_2$, (c) $NaGd_{0.8}(MoO_4)_2:Eu_{0.2}$, (d) $NaGd_{0.7}(MoO_4)_2:Eu_{0.1}Yb_{0.2}$ and (e) $NaGd_{0.5}(MoO_4)_2:Eu_{0.05}Yb_{0.45}$ particles. The diffraction patterns of the products can be assigned to the standard data of $NaGd(MoO_4)_2$ (JCPDS28-0828). No impurity phases were detected. $NaGd(MoO_4)_2$ as a member of double molybdate family has a sheelite structure with the tetragonal with space group $I4_{1/a}$[15]. In $NaGd(MoO_4)_2$ matrix, Na^+ and Gd^{3+} are randomly arranged and form a disordered structure. Eu^{3+} and Yb^{3+} ions can be effectively doped in the $NaGd(MoO_4)_2$ lattice by partial substitution of Gd^{3+} site due to the similar radii of Gd^{3+}, Eu^{3+} and Yb^{3+}. Post heat-treatment plays an important role in a well-defined crystallized morphology. To achieve a well-defined crystalline morphology, $NaGd(MoO_4)_2$, $NaGd_{0.8}(MoO_4)_2:Eu_{0.2}$, $NaGd_{0.7}(MoO_4)_2:Eu_{0.1}Yb_{0.2}$ and $NaGd_{0.5}(MoO_4)_2:Eu_{0.05}Yb_{0.45}$ phases need to be heat treated at 900 °C for 16 h. It is assumed that the doping amount of Eu^{3+}/Yb^{3+} has a great effect on the crystalline cell volume of the $NaGd(MoO_4)_2$, because of the different ionic sizes and energy band gaps.

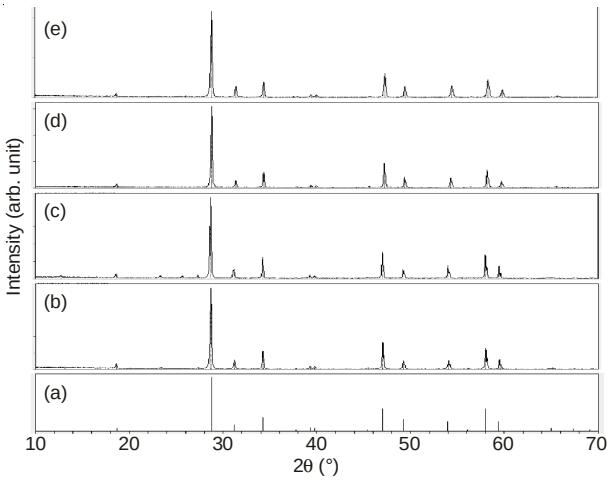

Fig. 1. X-ray diffraction patterns of the (a) JCPDS 25-0828 data of $NaGd(MoO_4)_2$, the synthesized (b) $NaGd(MoO_4)_2$, (c) $NaGd_{0.8}(MoO_4)_2:Eu_{0.2}$, (d) $NaGd_{0.7}(MoO_4)_2:Eu_{0.1}Yb_{0.2}$, and (e) $NaGd_{0.5}(MoO_4)_2:Eu_{0.05}Yb_{0.45}$ particles

Fig. 2 shows a SEM image of the synthesized $NaGd_{0.5}(MoO_4)_2:Eu_{0.05}Yb_{0.45}$ particles. The as-synthesized samples are well crys-

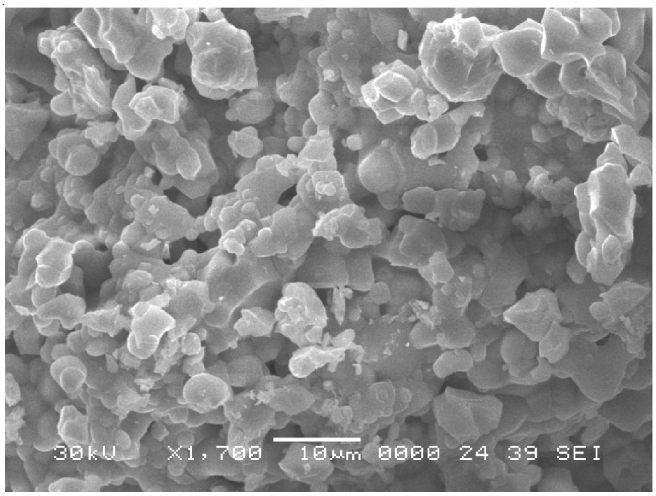

Fig. 2. Scanning electron microscopy image of the synthesized $NaLa_{0.5}(MoO_4)_2:Eu_{0.05}Yb_{0.45}$ particles

tallized with a fine and homogeneous morphology and particle size of 2-5 µm. It is noted that the obtained sample possesses a partial substitution of Gd^{3+} by Eu^{3+} and Yb^{3+} ions and the ions are effectively doped into crystal lattices of the $NaLa(MoO_4)_2$ phase due to the similar radii of Gd^{3+} and by Eu^{3+} and Yb^{3+}. This suggests that the cyclic microwave-modified sol-gel route is suitable for the growth of $NaGd_{1-x}(MoO_4)_2:Eu^{3+}/Yb^{3+}$ crystallites.

Fig. 3 shows the energy-dispersive X-ray spectroscopy patterns of the synthesized (a) $NaGd_{0.8}(MoO_4)_2:Eu_{0.2}$ and (b) $NaGd_{0.5}(MoO_4)_2:Eu_{0.05}Yb_{0.45}$ particles and quantitative compositions of (c) $NaGd_{0.8}(MoO_4)_2:Eu_{0.2}$ and (d) $NaGd_{0.5}(MoO_4)_2:Eu_{0.05}Yb_{0.45}$ particles. The EDS pattern shows that the (a) $NaGd_{0.8}(MoO_4)_2:Eu_{0.2}$ and (b) $NaGd_{0.5}(MoO_4)_2:Eu_{0.05}Yb_{0.45}$ particles are composed of Na, Gd, Mo, O and Eu for $NaGd_{0.8}(MoO_4)_2:Eu_{0.2}$ and Na, Gd, Mo, O, Eu and Yb for $NaGd_{0.5}(MoO_4)_2:Eu_{0.05}Yb_{0.45}$ particles. The quantitative compositions of (c) and (d) are in good relation with nominal compositions of the particles. The relation of Na, Gd, Mo, O, Eu and Yb components exhibits that $NaGd_{0.8}(MoO_4)_2:Eu_{0.2}$ and $NaGd_{0.5}(MoO_4)_2:Eu_{0.05}Yb_{0.45}$ particles can be successfully synthesized using the microwave-modified sol-gel method. The microwave-modified sol-gel process of double molybdates provides the energy to synthesize the bulk of the material uniformly, so that fine particles with controlled morphology can be fabricated in a short time period.

(a)

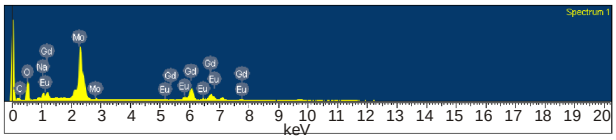

(b)

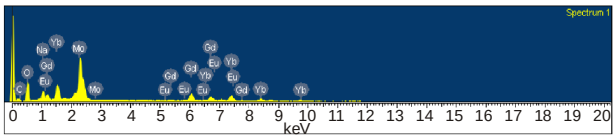

(c)

Spectrum	In stats.	C	O	Na	Mo	Eu	Gd	Total
Spectrum 1	Yes	9.91	35.73	2.22	30.70	2.83	18.61	100.00
Spectrum 2	Yes	8.11	36.14	2.60	31.33	3.06	18.76	100.00
Spectrum 3	Yes	8.02	36.81	2.26	31.15	3.12	18.64	100.00
Spectrum 4	Yes	7.49	36.61	2.28	32.05	2.98	18.59	100.00
Mean		8.38	36.32	2.34	31.31	3.00	18.65	100.00
Std. deviation		1.05	0.48	0.17	0.56	0.13	0.07	
Max.		9.91	36.81	2.60	32.05	3.12	18.76	
Min		7.49	35.73	2.22	30.70	2.83	18.59	

(d)

Spectrum	In stats.	C	O	Na	Mo	Eu	Gd	Yb	Total
Spectrum 1	Yes	9.44	35.13	3.29	27.39	0.50	11.22	13.04	100.00
Spectrum 2	Yes	8.93	34.70	3.29	27.89	0.28	11.26	13.65	100.00
Mean		9.19	34.91	3.29	27.64	0.39	11.24	13.34	100.00
Std. deviation		0.36	0.30	0.00	0.36	0.15	0.03	0.43	
Max.		9.44	35.13	3.29	27.89	0.50	11.26	13.65	
Min		8.93	34.70	3.29	27.39	0.28	11.22	13.04	

Fig. 3. Energy-dispersive X-ray spectroscopy patterns of the synthesized (a) $NaGd_{0.8}(MoO_4)_2:Eu_{0.2}$ and (b) $NaGd_{0.5}(MoO_4)_2:Eu_{0.05}Yb_{0.45}$ particles, and quantitative compositions of (c) $NaGd_{0.8}(MoO_4)_2:Eu_{0.2}$ and (d) $NaGd_{0.5}(MoO_4)_2:Eu_{0.05}Yb_{0.45}$ particles

Fig. 4 shows the upconversion photoluminescence emission spectra of the as-prepared (a) $NaGd(MoO_4)_2$, (b) $NaGd_{0.8}(MoO_4)_2:Eu_{0.2}$, (c) $NaGd_{0.7}(MoO_4)_2:Eu_{0.1}Yb_{0.2}$ and (d) $NaGd_{0.5}(MoO_4)_2:Eu_{0.05}Yb_{0.45}$ particles excited under 980 nm at room temperature. In the case of $NaGd_{0.7}(MoO_4)_2:Eu_{0.1}Yb_{0.2}$ particles, the upconversion intensity showed a strong 475 nm emission band in the blue region and a strong 525 nm and a weak 550 nm emission bands in the green region. In the case of $NaGd_{0.5}(MoO_4)_2:Eu_{0.05}Yb_{0.45}$ particles, the upconversion intensity exhibited a strong 525 nm emission band and a weak 550 nm emission band in the green region and a very weak 615 nm emission band in the red region. The strong 475 nm emission in the blue region corresponds to the $^7F_0 \rightarrow {}^5D_2$ transition. The strong 525 nm emission in the green region corresponds to the $^7F_0 \rightarrow {}^5D_1$ transition and the weak emission 550 nm band in the green region corresponds to the $^5D_1 \rightarrow {}^7F_J$ transition, while the very weak emission 615 nm band in the red region corresponds to the $^5D_0 \rightarrow {}^7F_2$ transition[16,17]. The upconversion intensities of (a) $NaGd(MoO_4)_2$ and (b) $NaGd_{0.8}(MoO_4)_2:Eu_{0.2}$ were not detected. The upconversion intensity of (d) $NaGd_{0.5}(MoO_4)_2:Eu_{0.05}Yb_{0.45}$ at 525 nm emission band is much higher than that of (c) $NaGd_{0.7}(MoO_4)_2:Eu_{0.1}Yb_{0.2}$ particles. The doping amounts of Eu^{3+}/Yb^{3+} had a great effect on the morphological features of the particles and their upconversion fluorescence intensity. The Yb^{3+} ion sensitizer can be effectively excited by the energy of an incident light source, this energy is transferred to the activator where radiation can be emitted. The Eu^{3+} ion activator is the luminescence center for these upconversion particles and the sensitizer Yb^{3+} enhances the upconversion luminescence efficiency.

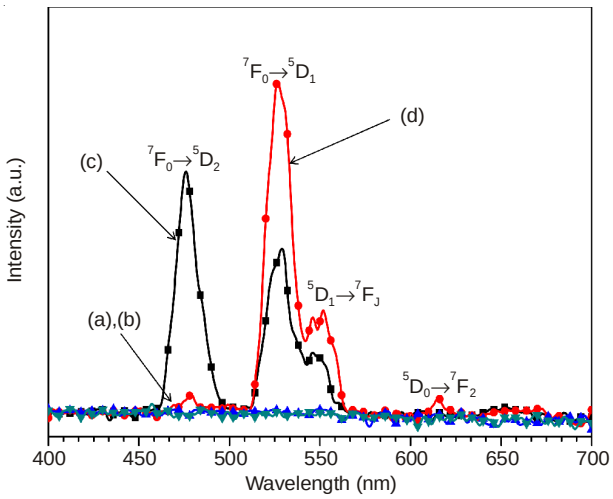

Fig. 4. Upconversion photoluminescence emission spectra of (a) $NaGd(MoO_4)_2$, (b) $NaGd_{0.8}(MoO_4)_2:Eu_{0.2}$, (c) $NaGd_{0.7}(MoO_4)_2:Eu_{0.1}Yb_{0.2}$ and (e) $NaGd_{0.5}(MoO_4)_2:Eu_{0.05}Yb_{0.45}$ particles excited under 980 nm at room temperature

Fig. 5 shows the Raman spectra of the synthesized (a) $NaGd(MoO_4)_2$ (NGM), (b) $NaGd_{0.5}(MoO_4)_2:Eu_{0.05}Yb_{0.45}$ (NGM:Eu), (c) $NaGd_{0.7}(MoO_4)_2:Eu_{0.1}Yb_{0.2}$ (NGM:EuYb) and (d) $NaGd_{0.5}(MoO_4)_2:Eu_{0.05}Yb_{0.45}$ (NGM:EuYb#) particles excited by the 514.5 nm line of an Ar ion laser at 0.5 mW. The internal modes for the pure $NaGd(MoO_4)_2$ (NLM) particles in Fig. 5(a) were detected at 323, 394, 818, 892, 994 and 1333 cm^{-1}, respectively. The well-resolved sharp peaks for the $NaGd(MoO_4)_2$ (NGM) particles indicate a high crystallinity state of the synthesized particles. The internal vibration mode frequencies are dependent on the lattice parameters and the degree of the partially covalent bond between the cation and molecular ionic group $[MoO_4]^{2-}$. The Raman spectra of the doped particles in Fig. 5(b), (c) and (d) indicated the domination of strong peaks at higher frequencies of 780, 890, 1366 and 1438 cm^{-1} and at lower frequencies of 324 and 400 cm^{-1}. The doped particles prove that the doping ions can influence the structure of the host materials. The combination of a heavy metal cation and the inter-ionic distance for Eu^{3+} and Yb^{3+} substitutions in Gd^{3+} sites in the lattice result in a high probability of upconversion and phonon-splitting relaxation in $NaGd_{1-x}(MoO_4)_2:Eu^{3+}/Yb^{3+}$ crystals. It is assumed that these very strong and strange effects are generated by the disorder of the $[MoO_4]^{2-}$ groups with the incorporation of the Eu^{3+} and Yb^{3+} elements into the crystal lattice or by a new phase formation[18].

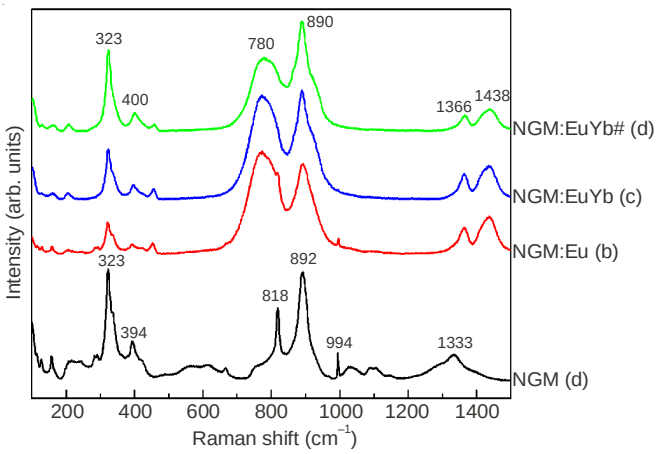

Fig. 5. Raman spectra of the synthesized (a) $NaGd(MoO_4)_2$(NGM), (b) $NaGd_{0.5}(MoO_4)_2:Eu_{0.05}Yb_{0.45}$(NGM:Eu), (c) $NaGd_{0.7}(MoO_4)_2:Eu_{0.1}Yb_{0.2}$(NGM:EuYb) and (d) $NaGd_{0.5}(MoO_4)_2:Eu_{0.05}Yb_{0.45}$ (NGdM:EuYb#) particles excited by the 514.5 nm line of an Ar ion laser at 0.5 mW

Conclusion

$NaGd_{1-x}(MoO_4)_2:Eu^{3+}/Yb^3$ phosphors with doping concentrations of Eu^{3+} and Yb^{3+} ($x = Eu^{3+} + Yb^{3+}$, $Er^{3+} = 0.05$, 0.1, 0.2 and $Yb^{3+} = 0.2$, 0.45) were successfully synthesized by the microwave-modified sol-gel method showing a fine and homogeneous morphology with particle sizes of 2-5 μm. In the case of $NaGd_{0.7}(MoO_4)_2:Eu_{0.1}Yb_{0.2}$ particles, the upconversion intensity showed a strong 475 nm emission band ($^7F_0 \rightarrow {}^5D_2$ transition) in the blue region and a strong 525 nm ($^7F_0 \rightarrow {}^5D_1$ transition) and a weak 550 nm ($^5D_1 \rightarrow {}^7F_J$ transition) emission bands in the green region. In the case of $NaGd_{0.5}(MoO_4)_2:Eu_{0.05}Yb_{0.45}$ particles, the upconversion intensity exhibited a strong 525 nm ($^7F_0 \rightarrow {}^5D_1$ transition) emission band and a weak 550 nm ($^5D_1 \rightarrow {}^7F_J$ transition) emission band in the green region and a very weak 615 nm ($^5D_0 \rightarrow {}^7F_2$ transition) emission band in the red region. The Raman spectra of the doped particles indicated the domination of strong peaks at higher frequencies of 780, 890, 1366 and 1438 cm^{-1} and at lower frequencies of 324 and 400 cm^{-1} induced by the disorder of the $[MoO_4]^{2-}$ groups with the incorporation of the Eu^{3+} and Yb^{3+} elements into the crystal lattice or by a new phase formation[15].

ACKNOWLEDGEMENTS

This study was supported by the Basic Science Research Program through the National Research Foundation of Korea (NRF) funded by the Ministry of Science, ICT & Future Planning (2014-046024).

REFERENCES

1. F. Mo, L. Zhou, Q. Pang, F. Gong and Z. Liang, *Ceram. Int.*, **38**, 6289 (2012).
2. C. Guo, T. Chen, L. Luan, W. Zhang and D. Huang, *J. Phys. Chem. Solids*, **69**, 1905 (2008).
3. M. Wang, G. Abbineni, A. Clevenger, C. Mao and S. Xu, *Nanomedicine*, **7**, 710 (2011).
4. C. Guo, H.K. Yang and J.H. Jeong, *J. Lumin.*, **130**, 1390 (2010).
5. J. Liao, D. Zhou, B. Yang, R. Liu, Q. Zhang and Q. Zhou, *J. Lumin.*, **134**, 533 (2013).
6. J. Sun, J. Xian and H. Du, *J. Phys. Chem. Solids*, **72**, 207 (2011).
7. T. Li, C. Guo, Y. Wu, L. Li and J.H. Jeong, *J. Alloys Comp.*, **540**, 107 (2012).
8. M. Nazarov and D.Y. Noh, *J. Rare Earths*, **28**, 1 (2010).
9. J. Sun, W. Zhang, W. Zhang and H. Du, *Mater. Res. Bull.*, **47**, 786 (2012).
10. J. Yao, Z. Jia, P. Zhang, C. Shen, J. Wang, K.F. Aguey-Zinsou, C. Ma and L. Wang, *Ceram. Int.*, **39**, 2165 (2013).
11. Z. Xia, H. Du, J. Sun, D. Chen and X. Wang, *Mater. Chem. Phys.*, **119**, 7 (2010).
12. F. Wu, L. Wang, C. Wu and Y. Bai, *Electrochim. Acta*, **54**, 4613 (2009).
13. S. Das, A.K. Mukhopadhyay, S. Datta and D. Basu, *Bull. Mater. Sci.*, **32**, 1 (2009).
14. C.S. Lim, *Mater. Chem. Phys.*, **140**, 154 (2013).
15. J. Liao, H. Huang, H. You, X. Qiu, Y. Li, B. Qiu and H. Wen, *Mater. Res. Bull.*, **45**, 1145 (2010).
16. J. Sun, J. Xian, X. Zhang and H. Du, *J. Rare Earths*, **29**, 32 (2011).
17. Q. Sun, X. Chen, Z. Liu, F. Wang, Z. Jiang and C. Wang, *J. Alloys Comp.*, **509**, 5336 (2012).
18. C.S. Lim, *Mater. Res. Bull.*, **48**, 3805 (2013).